
Article:
Ciuchi, IV, Chung, CC, Fancher, CM et al. (5 more authors) (2017) Field-induced antiferroelectric to ferroelectric transitions in (Pb1–xLax)(Zr0.90Ti0.10)1–x/4O3 investigated by in situ X-ray diffraction. Journal of the European Ceramic Society, 37 (15). pp. 4631-4636. ISSN 0955-2219

https://doi.org/10.1016/j.jeurceramsoc.2017.06.018

Field-induced antiferroelectric to ferroelectric transition in $(Pb_{1-x}La_x)(Zr_{0.90}Ti_{0.10})_{1-x/4}O_3$ investigated by in situ X-ray diffraction

I. V. Ciuchi,[1,2,a)] C. C. Chung,[3] C. M. Fancher,[4] J. Guerrier,[3] J. S. Forrester,[5] J. L. Jones,[3] L. Mitoseriu[2] and C. Galassi[1]

[1]CNR-ISTEC, Istituto di Scienza e Tecnologia dei Materiali Ceramici, Via Granarolo 64, I-48018, Faenza, Italy

[2]Dielectrics, Ferroelectrics & Multiferroics group, Faculty of Physics, *"A. I. Cuza"* Univ, .Bv.Carol I, n. 11, 700506 Iasi, Romania

[3]Department of Materials Science and Engineering, North Carolina State University, Raleigh, NC, 27695, USA

[4]Neutron Scattering Science Directorate, Oak Ridge National Laboratory, Oak Ridge, Tennessee 37831, USA

[5]School of Chemical and Process Engineering, University of Leeds, Leeds, LS2 9JT, UK

Phase transitions and field-induced preferred orientation in (Pb1-xLax)(Zr0.90Ti0.10)1–x/4O3(PLZT x/90/10)ceramics upon electric field cycling using in situ X-ray diffraction were studied. The evolution of the {200}pc and {111}pc diffraction line profiles indicate that PLZT 4/90/10 and PLZT 3/90/10 compositions undergo an antiferroelectric (AFE)–ferroelectric (FE) phase switching. Both PLZT 4/90/10 and PLZT3/90/10 exhibit irreversible preferred orientation after experiencing the field-induced AFE-to-FE phase switching. An electric field-induced structure develops in both compositions which has a reversible character during the field decreasing in PLZT 4/90/10 and an irreversible character in PLZT 3/90/10. In addition, structural analysis of pre-poled PLZT 3/90/10 ceramics show that it is possible to induce consecutive FE-to-AFE and AFE-to-FE transitions when fields of reversed polarity are applied in sequence. The field range required to induce the AFE phase is broad, and the phase transition is kinetically slow. This kind of transition has rarely been reported before.

[a)]Author to whom correspondence should be addressed. Electronic mail: ioana.ciuchi@istec.cnr.it

1. Introduction

The study of antiferroelectric materials has recently become an active field in condensed-matter science,[1-6] mainly due to the field-induced antiferroelectric (AFE) to ferroelectric (FE) transition which may provide a broad range of applications.[4,6-10]AFEs do not exhibit macroscopic spontaneous polarization because the antiparallel orientation of neighboring dipoles oppose one another. An electric field of amplitude $E_{AFE\text{-}FE}$ can induce switching of antiparallel to a parallel dipolar alignment (first-order AFE-to-FE phase transition).[11] These changes are observed in the measured polarization vs. electric-field (P(E)) hysteresis loops. For an irreversible phase transition (i.e. an FE phase), a single P(E) is observed, whereas a double hysteresis loop is observed if FE phase reverts to the AFE state.[8,10,12-14] It has been hypothesized that AFEs cannot be macroscopically poled.[11] However, recent investigations have demonstrated that the AFE composition ($Pb_{0.99}Nb_{0.02}[(Zr_{0.57}Sn_{0.43})_{0.92}Ti_{0.08}]_{0.98}O_3$) with a field assisted AFE-to-FE transition remains in a stable FE phase after the field is removed.[13] Furthermore, it is possible to induce the AFE phase from previously induced and poled FE phases by applying an electric field of reverse polarity.[15-17] The AFE-to-FE phase transition is a complex phenomenon, which includes structural phase transformations, unit cell volume changes, domain switching and texture formation.[5,13-16,18-22] The AFE-to-FE transition has been reported using macroscopic studies,[12,23-25] however microscopic studies to date are scarce.[5,13-16,18- 22] There is much that can be learned from studying the structural evolution at various fields before, during and after the AFE-to-FE phase transition. AFE lead lanthanum zirconate titanate ($(Pb_{1-x}La_x)(Zr_{0.90}Ti_{0.10})_{1-x/4}O_3$ (PLZT x/90/10) ceramics have received increasing interest due to their composition dependent phase boundary region between rhombohedral and orthorhombic phases.[10,24-26,28] Due to the proximity of the FE/AFE phase boundary at $2<x<4$ at % of La, a structural transition from orthorhombic Pbam to rhombohedral R3c is expected in AFE PLZT x/90/10 compositions during the application of adequate $E_{AFE\text{-}FE}$ threshold ($15<E_{AFE\text{-}FE}<75$ kV/cm) electric field.[10]

The aim of this work is to study the structural evolution of the AFE, and field-induced FE phase using in situ X-ray diffraction (XRD) measurements. Two compositions have been selected for detailed examination due to their location on either side of, and close proximity to, the FE/AFE phase boundary: PLZT 4/90/10 with previously observed AFE macroscopic character and PLZT 3/90/10 with macroscopic FE character.[10]

2. Experimental

Polycrystalline PLZT ceramics were consolidated from powders produced by solid-state reaction and densified to ~95% relative density, as described previously,[24] and cut into thin rectangular shapes. P(E) hysteresis loops were measured in a

parallel plate capacitor configuration using a modified Sawyer-Tower circuit with a bipolar triangular wave with a frequency of 1 Hz. For the in situ XRD measurements, the top surfaces of the ceramics were polished with diamond paste (0.5 μm), and annealed at 650 °C for 2 h to recover the virgin state, and to minimize the residual stresses/strains induced by polishing. The bottom surface was covered by a silver painted electrode, while the top surfaces of the ceramics were sputtered with a 40 nm thick platinum electrode. The in situ XRD experiments were carried out on a PANalytical Empyrean diffractometer using Cu-K_α radiation. A custom-built, time-resolved XRD technique (similar to that shown in Ref. [29]) was used to determine in situ the structural changes under the application of cyclic electric fields. For each field cycle, 68 XRD patterns were measured during the application of a bipolar triangular wave (1200 s period), parallel to the thickness direction of the samples, and with maximum amplitudes exceeding the coercive field. The diffraction data were acquired using a step size of 0.013° 2θ and count time of 13 s per step. To visualize electric field induced changes, diffraction patterns are shown as surface plots. This type of display highlights structural changes with positive and negative electric fields. Diffraction data were analyzed using single peak fitting to extract the full width at half maximum (FWHM) of the 111_{pc} reflection.

3. Results and discussion

The preparation, density, crystalline structure, phase composition and microstructure of the PLZT 4/90/10 and PLZT 3/90/10ceramics were discussed in details in a previous paper [24]. Well densified ceramics were obtained with the density higher than 10.95% of the theoretical value. Previous X-ray diffraction studies per-formed at room temperature evidence that FE (R3c rhombohedral structure) and AFE (Pbam orthorhombic structure) phase coexist in the PLZT 3/90/10 ceramic while the PLZT 4/90/10 ceramic shows diffraction peaks consisted with orthorhombic AFE phase. As evidenced in Fig. 1(a) and (b) the investigated ceramics display bimodal grain size distribution with large grains of about 6–7 μm together with smaller ones of about 2 μm. PLZT 3/90/10 ceramic show predominantly coarse grains while PLZT 4/90/10 ceramic have mostly fine grain size.

The P(E) hysteresis loops for the first and second cycles for PLZT 4/90/10, and PLZT 3/90/10 are included in Figs. 1(a) and (b). Both compositions show a small (dP/dE) slope for low fields, indicating that are predominantly in the AFE phase in their virgin states. Then, the FE phase is induced, as observed by a sudden increase of polarization at $E_{AFE\text{-}FE\ virgin}$ forward switching field. Upon reducing the field from the maximum value of 75 kV/cm, the polarization of the PLZT 4/90/10 sample reverts to 0 when the threshold field $E_{FE\text{-}AFE}$ ~27 kV/cm is reached (Fig. 1(a)), signifying that this composition exhibits a reversible AFE-to-FE field induced transition. In contrast, as indicated by a remanent polarization P_r of 30 μC/cm^2 and a single

P(E) loop during the second field cycle, the PLZT 3/90/10 composition remains polarized and the induced FE state is preserved, i.e. evidencing an irreversible AFE-to-FE field-assisted phase transition (Fig. 1(b)). It is widely accepted that typical AFE double hysteresis loops indicate the reversibility of AFE-to-FE field-induced transition (e.g., as shown in the final cycle of PLZT 4/90/10). It is worth mentioning that $E_{AFE\text{-}FE\ virgin}$ =68 kV/cm threshold value determined from minor cycles is higher than $E_{AFE\text{-}FE}$ =60 kV/cm corresponding to the last cycle (Fig. 1(a)), suggesting that the AFE phase is slightly destabilized during the electrical cycling. Hence, the strict reversibility of the AFE-to-FE phase transition and recovery of the initial AFE state after the field removal is thus called into question for the composition PLZT 4/90/10.

The sensitivity of XRD to crystallographic changes and modifications of domain structure and lattice strain,[30-32] have allowed the extraction of additional information about the AFE-to-FE transition.. The effect of field cycling on the structural evolution during the reversible/irreversible field induced AFE-to-FE transitions in PLZT 4/90/10 and PLZT 3/90/10 is explored. In their virgin states, PLZT 4/90/10 shows a Pbam orthorhombic structure while PLZT 3/90/10 has mixed Pbam orthorhombic and R3c rhombohedral phases.[24-25] Since the Pbam ground state is close in energy to a rhombohedral R3c phase,[33] a structural transition from Pbam to R3c is expected in these compositions during AFE-to-FE switching. This transition should manifest itself as significant changes in the appearance of the $\{111\}_{pc}$ and $\{200\}_{pc}$ pseudocubic diffraction line profiles. The 111_{pc} reflection should appear split in an XRD pattern containing a rhombohedral phase and unsplit if an orthorhombic phase is present, while the 200_{pc} reflection shows a single peak in an XRD pattern containing a rhombohedral structure and two $200_{pc}/002_{pc}$ reflections if the orthorhombic phase is present. Thus the evolution of the $\{111\}_{pc}$ and $\{200\}_{pc}$ diffraction line profiles was monitored in detail during the application of electric fields.

Figure 2 shows XRD patterns of PLZT 4/90/10. The diffraction intensity between $37°<2\theta<38°$ corresponds to the $\{111\}_{pc}$ diffraction line profile, while the diffraction intensity between $43°<2\theta<44°$ corresponds to the $002_{pc}/200_{pc}$ reflections of PLZT. At zero field, the $\{200\}_{pc}$ diffraction line profile is split into two, while the $\{111\}_{pc}$ is single, consistent with orthorhombic symmetry, as reported for this composition in the virgin state.[24-25] With increasing electric field, the 111_{pc} and 200_{pc} features are stable until $E=E_{AFE\text{-}FE\ virgin}$. As shown in Figs. 2(a) and (c), the $\{111\}_{pc}$ and $\{200\}_{pc}$ diffraction line profiles change when the threshold field $E_{AFE\text{-}FE\ virgin}$ = 68 kV/cm is reached. As evidenced by the simultaneous and instantaneous shift in position of the $\{111\}_{pc}$ diffraction line profile and the interchange between the intensity of the 200_{pc} and 002_{pc} reflections, a AFE-to-FE domain orientation is quickly induced. The shift towards lower 2θ of the $\{111\}_{pc}$ diffraction line profile is possibly due to non-uniform strains in the lattice caused by preferred orientation. The $\{111\}_{pc}$ diffraction line profile is asymmetric and not visibly split.

The initially single 200_{pc} reflection develops a distinct shoulder on the lower 2θ side (Fig. 2(d)). This indicates that, in addition to domain reorientation, the initial orthorhombic PLZT 4/90/10 undergoes a field-induced transformation to a lower symmetry phase (Fig. 2(d)). The structure of the field-induced phase cannot be determined here, but it is apparent that it has FE character, according to the associated P(E) loops. With decreasing the field from 74 kV/cm, the $\{111\}_{pc}$ and $\{200\}_{pc}$ diffraction line profiles return to the initial position when the field amplitude $E_{AFE\text{-}FE}$ = 28 kV/cm is reached, indicating that the orthorhombic structure has been recovered. Hence, the AFE-to-FE phase transition is quite reversible. However, after exposure to a field E = 74 kV/cm, the intensity of 200_{pc} AFE reflection remains significantly weaker while the intensity of 002_{pc} is increased. This intensity change indicates 90º domain reorientation, as previously found in tetragonal perovskite phases.[5,34,35] It is considered that the change in $002_{pc}/002_{pc}$ intensity of the AFE phase after the field-induced phase transition is related to strain-driven preferred orientation. This effect is maintained during the second cycle (Fig. 2(b)) which suggests that the high field FE state does not return to its AFE virgin state, but to an oriented AFE state. The AFE-to-FE switching is not fully reversible. Furthermore, from Figs. 2(a) and (b) it can be observed that the $E_{AFE\text{-}FE}$ = 60 kV/cm in the second cycle is lower than the $E_{AFE\text{-}FE\ virgin}$ = 68 kV/cm from first cycle, in agreement with the P(E) loops in Fig. 1(a) [indicated by $E_{AFE\text{-}FE\ virgin}$, and $E_{AFE\text{-}FE}$ in Fig. 1(a)]. This effect may be a consequence of the change in lattice strain and the domain switching which contributes to the macroscopic response of PLZT 4/90/10.

Figure 3 maps the field-dependence of the characteristic $\{111\}_{pc}$ and $\{200\}_{pc}$ pseudocubic diffraction line profiles for the PLZT 3/90/10 composition, which, in the virgin state, is within the compositional range of AFE/FE coexistence.[24-25] At E = 0, the doublet $\{200\}_{pc}$ and the single $\{111\}_{pc}$ diffraction line profiles suggest that the majority phase is orthorhombic. When the field amplitude of $E_{AFE\text{-}FE\ virgin}$ = 24 kV/cm is reached, PLZT 3/90/10 exhibits AFE-to-FE switching similar to PLZT 4/90/10, i.e., the 111_{pc} reflection shifts to a lower 2θ while the $\{200\}_{pc}$ doublet merges into a single reflection. The features of the 111_{pc} and 200_{pc} reflections in the high field FE phase are preserved when the field is returned to zero. The XRD results clearly illustrate the irreversible character of the AFE-to-FE transition in PLZT 3/90/10.

Interestingly, upon reversing the field polarity in the third quarter of the first field cycle, a partial recovery of the 111_{pc} and 200_{pc} AFE specific reflection position and features is observed for an electric field of ~-6 kV/cm. This indicates a field-assisted FE-to-AFE phase transition, within a limited field range (0-6 kV/cm) of negative polarity. The FE-to-AFE field-induced transition is uncommon, since it is widely accepted that an electric field favors the FE phase with parallel dipoles over the AFE phase. However, anomalies which confirm the recovery of AFE are not observed in the P(E) loop (Fig. 1(b)). Hence, in order to verify the occurrence of the field-induced FE-to-AFE phase transition, in situ XRD measurements were performed during the second electric cycle by applying a field with the same amplitude but reversed polarity. As indicated in Figs. 3(b) and (d),

the 111_{pc} and 200_{pc} AFE phase signature XRD reflections reappear during the first and the third quarter of the second cycle, showing the highest amplitude at the same coercive field (E_{FE-AFE} = ~6 kV/cm), thus confirming the re-appearance of the AFE phase from the FE phase. The fact that the experimental P(E) loop for PLZT 3/90/10 measured during the first and second field cycles do not show evidence of this field-induced FE-to-AFE transition may be explained by considering that the frequency of 1 Hz is significantly different to that used in the in situ XRD measurements (0.8 mHz). Therefore, an ultralow frequency is required to induce such an AFE-to-FE transition. A similarly induced AFE state originating from an FE phase was previously observed in $NaNbO_3$-based lead-free and $Pb_{0.99}\{Nb_{0.02}[(Zr_{0.57}Sn_{0.43})_{1-y}Ti_y]_{0.98}\}O_3$ ceramics.[14-15]

An analysis of the FWHM of the 111_{pc} reflection in the vicinity of the FE-to-AFE field induced transition (Fig. 4) was performed. The FWHM increases during the application of field with reversed polarity and it shows a prominent maximum for E~6 kV/cm. A larger FWHM may be associated with a transition to a new phase, and in this case, the FE-to-AFE phase. The AFE-to-FE phase transition is not completed instantly at a specific threshold field, but rather it occurs throughout a broad field range, and therefore the field-induced FE-to-AFE phase transition has slow kinetics and a diffuse character. Therefore, a key factor to induce an FE-to-AFE phase transition is to expose a poled FE phase to a reverse polarity field of small to moderate amplitude for a long time. At weak electric fields of reverse polarity, volume contraction due to the negative longitudinal strain may play a role in this process. Further field increases result in a reduction in the 111_{pc} FWHM while the 002_{pc} reflection decreases. These changes are consistent with the high field FE phase and thus, the induced AFE phase is returned to the FE phase at a field E >11 kV/cm. It is observed that the threshold field E_{AFE-FE} ~10 kV/cm is significantly lower than the coercive $E_{AFE-FE\ virgin}$ = 24 kV/cm field for the virgin state. In addition, this field level is almost identical to the coercive field E_c of the induced FE phase (Fig. 1(b), second cycle).

4. Conclusions

In summary, in situ X-ray diffraction measurements under the application of electric field reveal that an irreversible oriented domain structure and a field-induced FE reversible/irreversible structure are developed during AFE-to-FE switching in PLZT 4/90/10 and PLZT 3/90/10 ceramics. In addition, XRD results evidence FE-to-AFE and AFE-to-FE consecutive transitions when a field of reversed polarity is applied on previously poled 3/90/10 composition.

Acknowledgments

The authors thank C. Capiani (ISTEC) for the skillful preparation of the samples. The support from COST Action MP1308 is acknowledged. This work was performed in part at the Analytical Instrumentation Facility (AIF) at North Carolina State

University, which is supported by the State of North Carolina and the National Science Foundation (award number ECCS-1542015). The AIF is a member of the North Carolina Research Triangle Nanotechnology Network (RTNN), a site in the National Nanotechnology Coordinated Infrastructure (NNCI).

[1] A. Y. Borisevich, E. A. Eliseev, A. N. Morozovska, C.-J. Cheng, J.-Y. Lin, Y. H. Chu, D. Kan, I. Takeuchi, V. Nagarajanand S. V. Kalinin, Nat. Commun. 3, 775 (2012).

[2] A. K. Tagantsev, K. Vaideeswaran, S. B. Vakhrushev, A. V. Filimonov, R. G. Burkovsky, A. Shaganov, D. Andronikova, A. I. Rudskoy, A. Q. R. Baron, H. Uchiyama, D. Chernyshov, A. Bosak, Z. Ujma, K. Roleder, A. Majchrowski, J.-H. Ko and N. Setter, Nat. Commun. 3, 775 (2012).

[3] X.-K. Wei, A. K. Tagantsev, A. Kvasov, K. Roleder, C.-L. Jia and N. Setter, Nat. Commun. 5, 3031 (2014).

[4] Z. Zuo, B. Chen, B. Wang, H. Yang, Q. Zhan, Y. Liu, J. Wang, and R.-W. Li, Sci. Rep. 5, 16164 (2015).

[5] T. Lu, A. J. Studer, L. Noren, W. Hu, D. Yu, B. McBride, Y. Feng, R. L. Withers, H. Chen, Z. Xu and Y. Liu, Sci. Rep. 6, 23659 (2016).

[6] S. Lisenkov, B. K. Mani, E. Glazkova, C. W. Miller and I. Ponomareva. Sci. Rep. 6, 19590 (2016).

[7] W.-H. Chan, Z. Xu, J. Zhai, and H. Chen, Appl. Phys. Lett. 87, 192904 (2005).

[8] A. Pathak, C. Prakash and R. Chatterjee, Physica B 404, 3457 (2009).

[9] K. Uchino, Actuators 5, 1 (2016).

[10] I. V. Ciuchi, L. Mitoseriu, and C. Galassi, J. Am. Ceram. Soc. 99, 2382 (2016).

[11] C. Kittel, Phys. Rev. B. 82, 729 (1951).

[12] P. Yang and D. A. Payne, J. Appl. Phys. 71, 1361 (1992).

[13] X. Liu and X. Tan, Appl. Phys. Lett. 107, 072908 (2015).

[14] J. Gao, Q. Li, Y. Li, F. Zhuo, Q. Yan, W. Cao, X. Xi, Y. Zhang, and X. Chu, Appl. Phys. Lett. 107, 072909 (2015).

[15] X. Tan, J. Frederick, C. Ma, W. Jo, and J. Rödel, Phys. Rev. Lett. 105, 255702 (2010).

[16]Y. Xu, W. Hong, Y. Feng, and X. Tan, Appl. Phys. Lett. 104, 052903 (2014).

[17] H. Guo and X. Tan, Phys. Rev. B 91, 144104 (2015).

[18] L. Shebanov, M. Kusnetsov, and A. Sternberg, J. Appl. Phys. 76, 4301 (1994).

[19] C. T. Blue, J. C. Hicks, S.-E. Park, S. Yoshikawa, and L. E. Cross, Appl. Phys. Lett. 68, 2942 (1996).

[20] S.-E. Park, M.-J. Pan, K. Markowski, S. Yoshikawa, and L. E. Cross, J. Appl. Phys. 82, 1798 (1997).

[21] Y. Yu and R. N. Singh, J. Appl. Phys. 94, 7250 (2003).

[22] I. Dutta and R. N. Singh, Integr. Ferroelectr. 131, 153 (2011).

[23] X. Tan, S. E. Young, Y. H. Seo, J. Y. Zhang, W. Hong, and K. G. Weber, Acta Mater. 62, 114 (2014).

[24] I. V. Ciuchi, F. Craciun, L. Mitoseriu, and C. Galassi, J. Alloy. Comp. 646, 16 (2015).

[25] F. Craciun, F. Cordero, I. V. Ciuchi, L. Mitoseriu, and C. Galassi, J. Appl. Phys. 117, 184103 (2015).

[26] A. Pelàiz-Barranco, R. Villaurrutia, J. de los Santos Guerra, and P. Saint-Gregoire, J. Am. Ceram. Soc. 1, 8 (2016).

[27] A. Peláiz-Barranco, Y. González-Abreu, Y. Gagou, P. Saint-Grégoire, and J. D. S. Guerra, Vib. Spectrosc. 86, 124 (2016).

[28] A. Peláiz-Barranco, J. Wang, and T. Yang, Ceram. Int. 42, 229 (2016).

[29] A. Pramanick and J. L. Jones, IEEE Trans. Ultrason. Ferroelectr. Freq. Control. 56, 1546 (2009).

[30] J. L. Jones, E. B. Slamovich, and K. J. Bowman, J. Appl. Phys. 97, 034113 (2005).

[31] J. L. Jones, M. Hoffman, J. E. Daniels, and A. J. Studer, Appl. Phys. Lett. 89, 092901 (2006).

[32] J. L. Jones, S. C. Vogel , E. B. Slamovich, and K. J. Bowman, Scr. Mater. 51, 1123 (2004).

[33] K. Roleder, G. E. Kugel, J. Handerek, M. D. Fontana, C. Carabatos, M. Hafin, and A. Kania, Ferroelectrics 80, 161 (1998).

[34] A. Pramanick, D. Damjanovic, J. E. Daniels, J. C. Nino, and J. L. Jones, J. Am. Ceram. Soc. 94, 293 (2011).

[35] J. L. Jones, E. B. Slamovich, and K. J. Bowman, J. Appl. Phys. 97, 034113 (2005).

Figure captions

FIG. 1. Two subsequent recorded hysteresis loops: Loop 1, for the virgin sample; Loop 2, determined during the second run at 1 Hz. "$E_{AFE\text{-}FE\ virgin}$" and "$E_{AFE\text{-}FE}$" indicate the forward switching field for inducing the AFE-to-FE transition during first cycle and second cycle respectively while "$E_{FE\text{-}AFE}$" indicate the forward switching field for the backward switching field of the FE-to-AFE recovery during first cycle and second cycle. (a) PLZT 4/90/10, and (b) PLZT 3/90/10.

FIG. 2. Contour plots of diffraction intensities for a) and b) $(002)_{pc}/(200)_{pc}$, and c) $(111)_{pc}$ reflections for the **PLZT 4/90/10** composition during a complete triangular field cycle with amplitude ±74 kV/cm and frequency 0.8 mHz during a) and c) first and b) second electrical cycle. The diffraction profiles from d) show the $(002)_{pc}/(200)_{pc}$ reflections before application of electric field (black), at the coercive field of -74 kV/cm (red) and after application of electric field (green). The subscript pc indicates reflections indexed with the pseudocubic primitive cell. A schematic drawing to describe the experimental sequence of applied electric field is included in the left hand side of the figure. $E_{AFE\text{-}FE}$ and $E_{FE\text{-}AFE}$ represent the forward switching field for inducing the AFE-to-FE transition and the backward switching field of the FE-to-AFE recovery, respectively.

FIG. 3. Contour plots of diffraction intensities for a) and b) $111_{pc}/\text{-}111_{pc}$, c) and d) $200_{pc}/002_{pc}$ reflections for the **PLZT 3/90/10** composition as a function of triangular bipolar electric field of ±45 kV/cm and frequency of 0.8 mHz during a) and c) first, and b) and d) second electrical cycle. The subscript pc indicates reflections indexed with the pseudocubic primitive cell. A schematic diagram to describe the experimental sequence of applied electric field is included on the left hand side of the figure. $E_{AFE\text{-}FE}$ and $E_{FE\text{-}AFE}$ represent the forward switching field for inducing the AFE-to-FE transition and the reverse switching field of the FE-to-AFE recovery, respectively.

FIG. 4. Electric field dependence of FWHM of the 111_{pc} reflection during the field-induced FE-to-AFE and AFE-to-FE transitions for the composition PLZT 3/90/10.

Figure 1

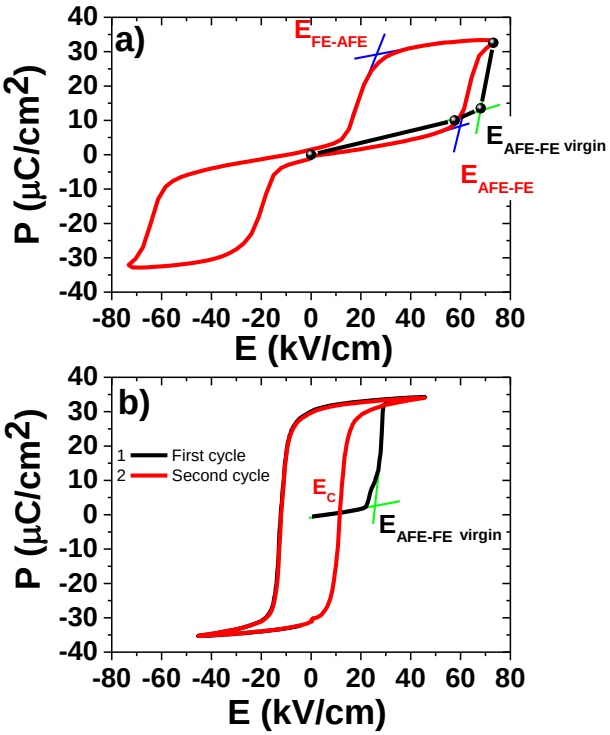
a)
E_{FE-AFE}
$E_{AFE-FE\ virgin}$
E_{AFE-FE}
P (μC/cm2)
E (kV/cm)
b)
1 First cycle
2 Second cycle
E_C
$E_{AFE-FE\ virgin}$
P (μC/cm2)
E (kV/cm)

Figure 2

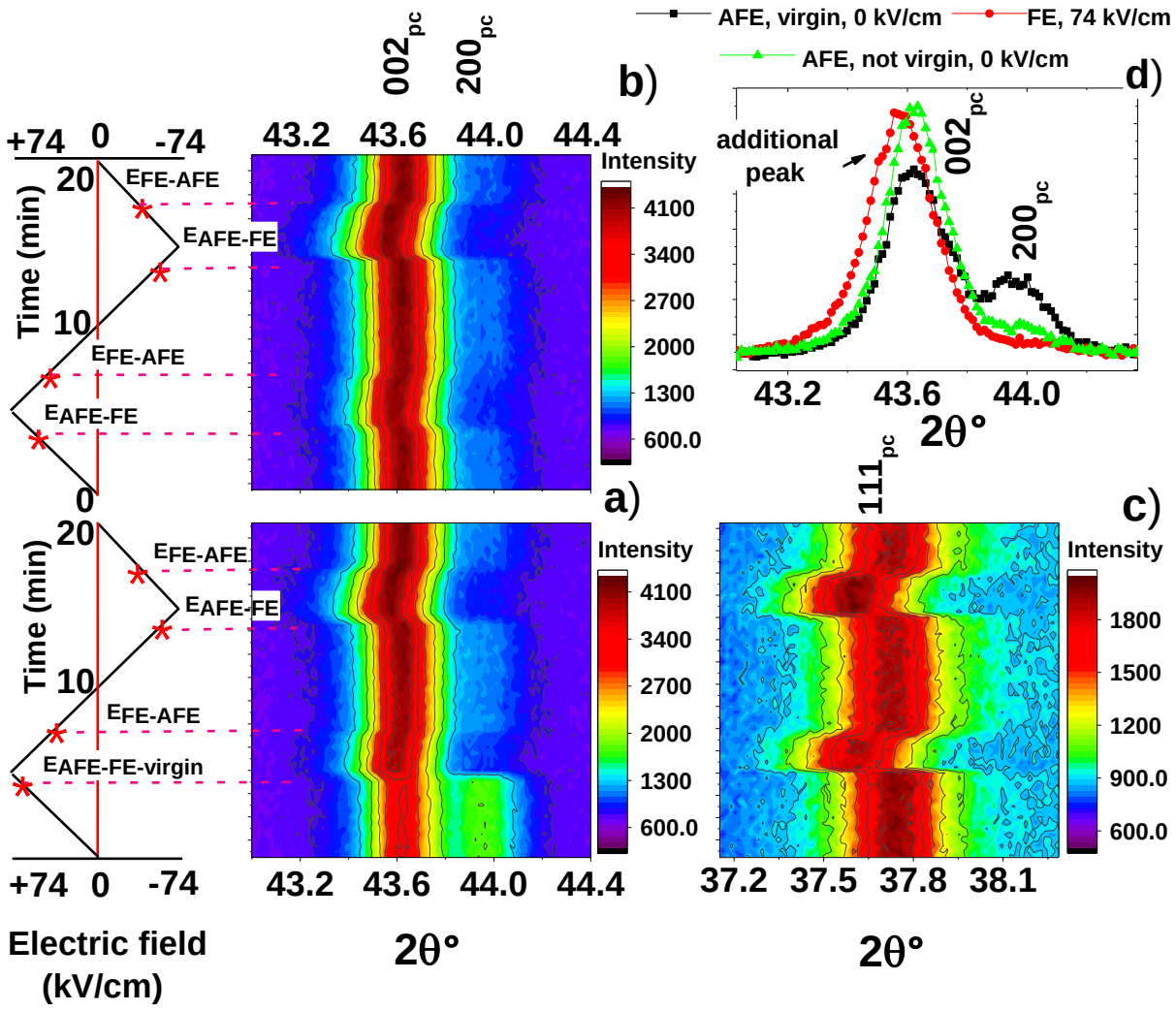
AFE, virgin, 0 kV/cm
FE, 74 kV/cm
AFE, not virgin, 0 kV/cm
d)
additional peak
002pc
200pc
111pc
b)
a)
c)
Intensity
Time (min)
EFE-AFE
EAFE-FE
EAFE-FE-virgin
+74 0 -74
Electric field (kV/cm)
2θ°

Figure 3

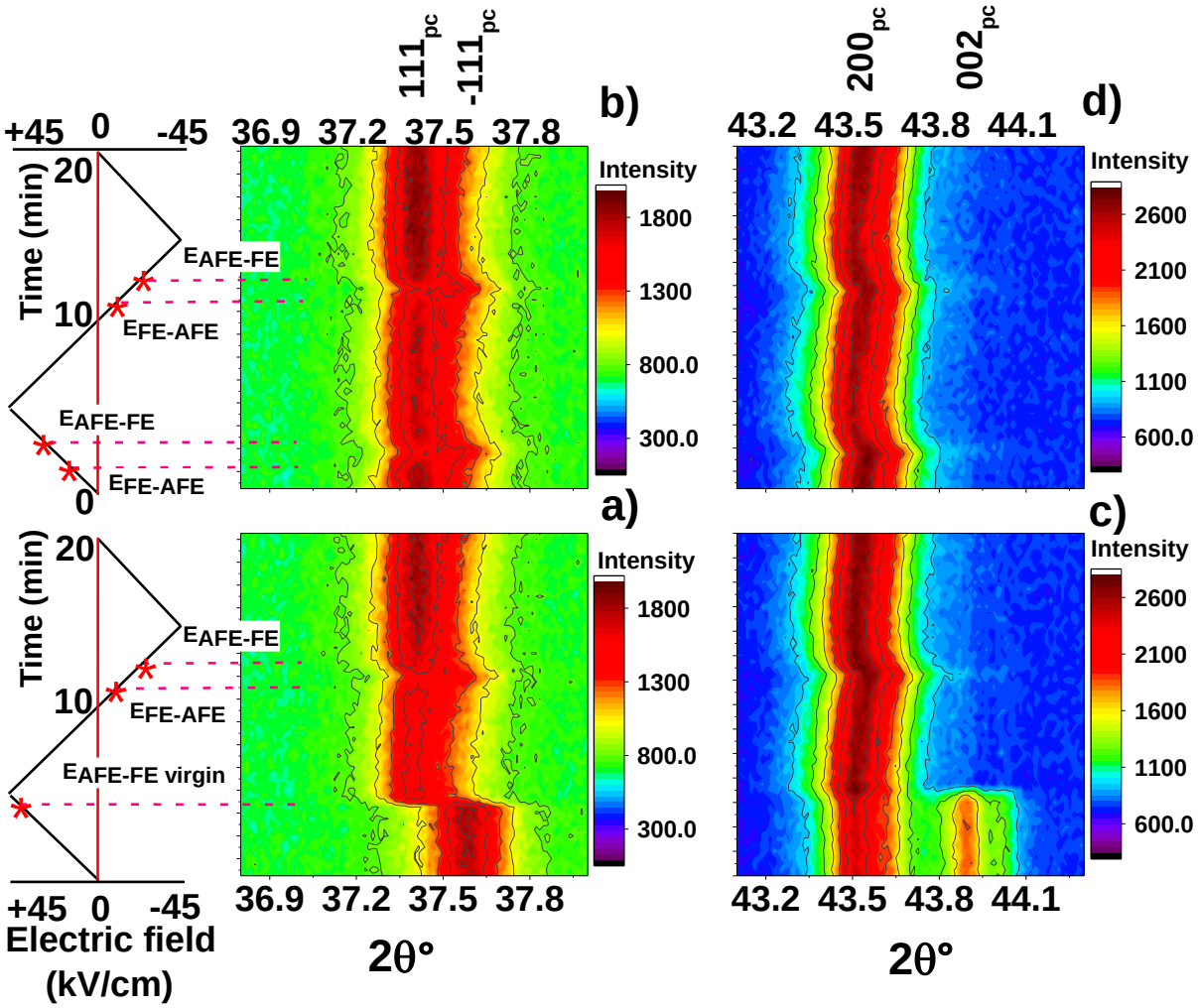
111pc
-111pc
200pc
002pc
b)
d)
a)
c)
+45 0 -45
36.9 37.2 37.5 37.8
43.2 43.5 43.8 44.1
Time (min)
20
10
0
EAFE-FE
EFE-AFE
EAFE-FE virgin
Intensity
1800
1300
800.0
300.0
2600
2100
1600
1100
600.0
Electric field
(kV/cm)
2θ°

Figure 4

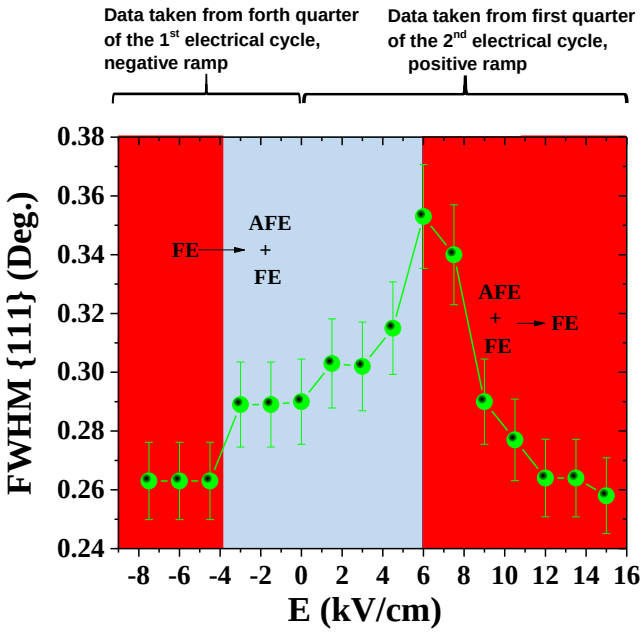
Data taken from forth quarter of the 1st electrical cycle, negative ramp
Data taken from first quarter of the 2nd electrical cycle, positive ramp
FE
AFE + FE
AFE + FE
FE
FWHM {111} (Deg.)
E (kV/cm)
0.38
0.36
0.34
0.32
0.30
0.28
0.26
0.24
-8 -6 -4 -2 0 2 4 6 8 10 12 14 16